

Analysis of different combining schemes of two amplify-forward relay branches with individual links experiencing Nakagami fading

Babu Sena Paul and Ratnajit Bhattacharjee

Abstract—Relay based communication has gained considerable importance in the recent years. In this paper we find the end-to-end statistics of a two hop non-regenerative relay branch, each hop being Nakagami- m faded. Closed form expressions for the probability density functions of the signal envelope at the output of a selection combiner and a maximal ratio combiner at the destination node are also derived and analytical formulations are verified through computer simulation. These density functions are useful in evaluating the system performance in terms of bit error rate and outage probability.

Keywords—co-operative diversity, diversity combining, maximal ratio combining, selection combining.

I. INTRODUCTION

Communication through cooperative relaying is emerging as an important technique in modern wireless systems. Wireless relaying allows mobile terminals to participate in the transmission of information, themselves not being the initial source or the final destination [1],[2]. Diversity is used to mitigate the effects of fading and therefore increasing the reliability of radio links in wireless networks. The main idea of cooperative diversity schemes is to use relay nodes as virtual antennas to facilitate the communication of a source-destination pair. Potential application areas of cooperation diversity include advanced cellular architectures, mobile wireless ad-hoc networks, and other hybrid networks in order to increase coverage, throughput, and capacity to transmit to the actual destination or next relay.

The relays of a cooperative diversity system can be broadly classified into two different categories depending on their functionalities. The relays are classified as either non-regenerative or regenerative type. The non-regenerative relays simply amplifies and forwards (A & F) the received signal to the next participating relay and/or the destination node. The complexity and latency of these type of relays are less as compared to the regenerative type. A regenerative relay decodes, encodes and then forwards the received signal to the next participating relay and/or the destination node. As the received signal requires to be decoded and encoded at the relay, the process proves to be computationally complex and time intensive. The non-regenerative relays are generally preferred when complexity and/or latency issues are important as these relays are usual

Babu Sena Paul is with the Indian Institute of Technology Guwahati, India, email: babusena_paul@yahoo.com

Ratnajit Bhattacharjee is with the Indian Institute of Technology Guwahati, India, email: ratnajit@iitg.ernet.in

battery powered and has limited processing capacities [3]. However, in a non-regenerative system, because of the presence of intermediate relay nodes, the statistics of the signal received at the destination depends on the channel conditions the signal experiences in the individual links. For properly utilizing the characteristics of a relay link in system design we require to understand the statistical behavior of such channels. Analysis of statistical behavior of relay channel has been a research area of considerable interest and recently some papers dealing with the methods of determining the statistics of such relay channels have appeared in the literature [3][5].

Mostly the individual relay links are assumed to be independent Rayleigh faded channels. In this communication we consider two-hop relay links, the individual links to be independent and but not necessarily identical Nakagami- m distributed but not necessarily identical. The Nakagami fading model is considered because of its flexibility of changing the individual link statistics by changing the parameter m [4].

The rest of the paper is organized as follows: In section 2 we discuss a two hop relay system. Section 3 deals with the diversity combining techniques, with reference to selection and maximal ratio combining in a relay based system. The simulation results are presented in section 4. Finally in section 5, we make the concluding remarks of the paper.

II. TWO HOP RELAY BASED SYSTEM

The simplest form of relay based communication is a two-hop communication link as shown in Fig. 1. The first hop is from the source node to the relay and the second is from the relay to the destination node. The source node may be a base station in case of advanced cellular architectures or a mobile station in a ad-hoc network.

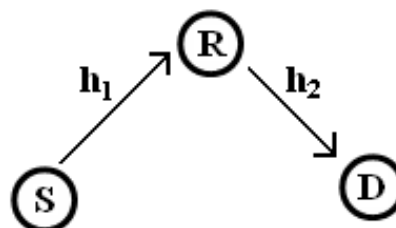


Fig. 1. A typical two hop relay based system.

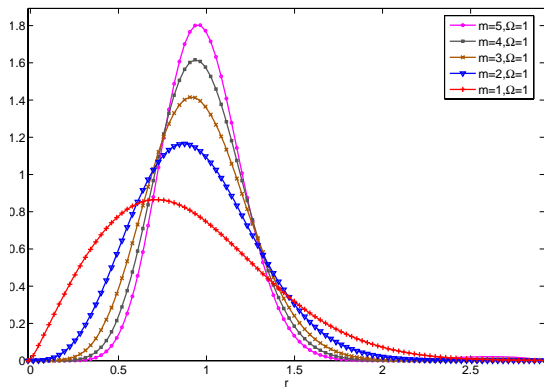


Fig. 2. The plot of Nakagami- m distribution for different values of m .

In the rest of the paper we assume the relay to be an ideal noise free repeater of non-regenerative type. Relays of non-regenerative types may be further classified into two different groups based on the type of amplification. A relay with constant amplification factor is said to be a fixed gain relay. For a variable gain relay, the amplification factor varies with time. For most cases, the variation depends on the variation of the channel. In our discussion we consider the relays to be of fixed gain type. The gain is assumed to be unity without any loss of generality. Assumption of noise free repeater simplifies analytical modeling. Subsequently, through simulation studies we estimate the maximum signal to noise ratio level at the relay at which the system bit error rate performance is not degraded exceeding a specified root mean square (RMS) error level.

In Fig. 1. the signal reaches the destination (D) from the source (S) via a relay node (R). $h_1(t)$ and $h_2(t)$ represent the channel between the S-R and R-D link respectively. As mentioned, $h_1(t)$ and $h_2(t)$ are modeled as Nakagami- m distributed so that various fading scenarios can be generated as particular cases of the generalized model. The probability density function (pdf) of the amplitudes of $h_1(t)$ and $h_2(t)$ may be written as [4]

$$f_{H_i}(h_i) = 2 \left(\frac{m_i}{\Omega_i} \right)^{m_i} \frac{h_i^{2m_i-1}}{\Gamma(m_i)} \exp \left(-\frac{m_i}{\Omega_i} h_i^2 \right) \quad (1)$$

where, $r_i > 1$ and $i=1,2$. $\Gamma(\cdot)$ represents the Gamma function. m_i denotes the m parameter of Nakagami- m distribution for the i^{th} hop. For $m=1$, we get the conventional Rayleigh fading model while by taking $m > 1$, the channel is made to behave more like a Rician channel. Fig. 2. shows the plot of Nakagami distribution for different values of m .

H_1 and H_2 are the random variables (RVs) representing the amplitudes of the links S-R and R-D respectively. m_1 and m_2 are the corresponding Nakagami- m parameters. In a typical 2-hop cooperative relaying environment, the source transmits the information in a time slot $\frac{T}{2}$ and the relay amplifies and retransmits the same information to the destination node in the next $\frac{T}{2}$ time slot. For the flat fading case the received signal

at the destination node may be written as,

$$y(t) = A(t) h_1(t) h_2(t) x(t) + A(t) h_2(t) n_1(t) + n_2(t) \quad (2)$$

for,

$$\frac{T}{2} \leq t \leq T$$

where,

$x(t)$ is the transmitted signal.

$A(t)$ is the gain of the relay.

$n_1(t)$ and $n_2(t)$ are the additive noise at the relay and the destination respectively.

As mentioned, for the sake of simplicity but without any loss of generality the relay is assumed to be a constant gain relay having an unity gain, i.e. $A(t)=1$. Moreover the relay is assumed to behave like a noise free repeater, thus $n_1(t)=0$. So (2) may be rewritten as,

$$y(t) = h_1(t) h_2(t) x(t) + n_2(t) \quad (3)$$

The effective channel between the source and the destination is basically the product of two Nakagami- m distributed RVs' and can be written as $Z = H_1 H_2$. The density function of the RV Z gives the channel statistics between the source and the destination via a relay. The density function of any RV obtained from the product of two independent RVs' is shown in [10].

$$f_Z(z) = \int_{-\infty}^{\infty} f_{H_1}(h_1) f_{H_2} \left(\frac{z}{h_1} \right) \frac{1}{|h_1|} dh_1 \quad (4)$$

where, f_{H_1} and f_{H_2} are the probability density functions of the independent random variables H_1 and H_2 respectively. As f_{H_1} and f_{H_2} are zero for $h_1 < 0$, hence the lower limit of (4) may be set to zero. From (1) and (4) we obtain,

$$f_Z(z) = \frac{4}{z \Gamma(m_1) \Gamma(m_2)} \left(\frac{z^2 m_1 m_2}{\Omega_1 \Omega_2} \right)^{\frac{m_1+m_2}{2}} K_{(m_1-m_2)} \left(2 \sqrt{\frac{z^2 m_1 m_2}{\Omega_1 \Omega_2}} \right) \quad (5)$$

where m_1 and m_2 are the Nakagami parameters of each hop and $K_\nu(\cdot)$ denotes the modified Bessel Function of second kind with order ν [6].

Fig.3. shows a comparison between the density function obtained analytically from (5) with the density function obtained from simulation of Nakagami- m distribution by employing techniques reported in literature [8]. In this technique samples of Nakagami distributed numbers with parameter m are generated from $2m$ number of independent and identically distributed (iid) Gaussian random variables. Ω for the Nakagami distributed random numbers is $2m\sigma_x^2$, where σ_x^2 gives the variance of the individual gaussian distributed RV's.

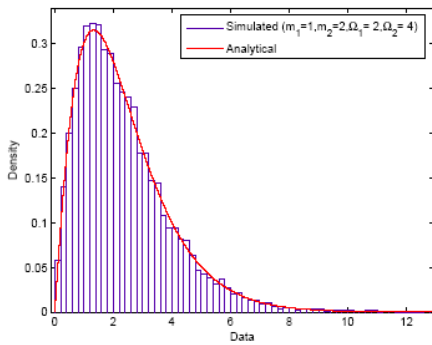


Fig. 3. The S-D channel statistics of a two hop relay system.

III. DIVERSITY COMBINING SCHEMES

Diversity combining is a very efficient receiver end technique for performance improvement of a wireless communication link. There are different methods of combining the received signals obtained by different diversity branches. These methods have a trade-off between complexity and performance. The most commonly used combining schemes are i) selection combining (SC), ii) maximal ratio combining (MRC), and iii) equal gain combining (EGC). In this paper we confine ourselves to the first two combining techniques. EGC can be considered as a special case of MRC.

In SC one of the L -diversity signals is selected for further processing. The diversity branch having the highest signal to noise ratio (SNR) or in an interference limited system, having the highest signal to co-channel interference ratio (SIR) is generally chosen. Measurement of SNR or SIR at the receiver is difficult, so the path having the highest power is chosen assuming that all the diversity paths are affected by the same noise power.

In MRC, the signals obtained at the receiver from different diversity branches are co-phased and the gain on each branch is set equal to the signal amplitude to the mean noise power ratio [9] Thus the branch weights are given by

$$w_i = a_i e^{j\theta_i} \quad i = 1, 2, \dots, L \quad (6)$$

where,

$$a_i = r_i / N_i \quad (7)$$

N_i is the mean noise power at the i^{th} branch.
 r_i is the received signal at the i^{th} branch.

In Fig. 4. we consider a scenario where it has been assumed that direct path between the source and the destination is blocked. The destination receives the signal only through the relay paths. The S-D link via relay R1 and that via relay R2 are assumed to be independent. $f_{Z_1}(z_1)$ and $f_{Z_2}(z_2)$ are therefore independent and gives the statistics of the S-D link via relay R1 and R2 respectively. The signal from the two relays are assumed to reach the destination in two orthogonal time slots, which are buffered for later processing.

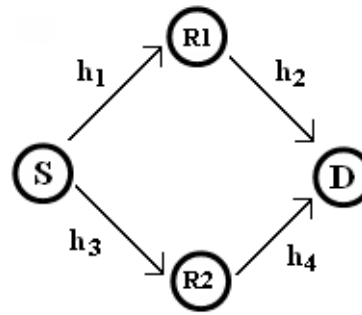


Fig. 4. Two branch dual hop relay diversity links.

The joint probability density function, $f_{Z_1 Z_2}(z_1 z_2)$, of the two independent relay channels may be written as,

$$f_{Z_1 Z_2}(z_1 z_2) = f_{Z_1}(z_1) f_{Z_2}(z_2) \quad (8)$$

So from (5) and (8),

$$f_{Z_1 Z_2}(z_1 z_2) = \frac{16}{z_1 z_2 \prod_{i=1}^4 \Gamma(m_i)} \left(\frac{z_1^2 m_1 m_2}{\Omega_1 \Omega_2} \right)^{\frac{m_1+m_2}{2}} \left(\frac{z_2^2 m_3 m_4}{\Omega_3 \Omega_4} \right)^{\frac{m_3+m_4}{2}} K_{(m_1-m_2)} \left(2\sqrt{\frac{z_1^2 m_1 m_2}{\Omega_1 \Omega_2}} \right) K_{(m_3-m_4)} \left(2\sqrt{\frac{z_2^2 m_3 m_4}{\Omega_3 \Omega_4}} \right) \quad (9)$$

where m_1, Ω_1 and m_2, Ω_2 represents the Nakagami distribution parameters of the wireless links S-R1 and R1-D respectively. Similarly m_3, Ω_3 and m_4, Ω_4 represents the same for the S-R2 and R2-D links respectively.

A. Selection Diversity

A two branch selection diversity system is shown in Fig. 5. The instantaneous SNR in terms of voltage, denoted as SNR_V , may be written as,

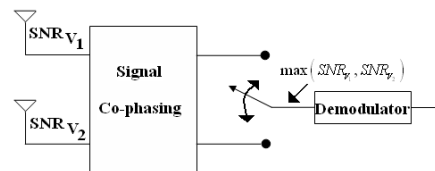


Fig. 5. The block diagram of a selection combiner.

$$SNR_{V_{sel}} = \frac{1}{\sqrt{N}} \max(z_1, z_2) \quad (10)$$

where z_1 and z_2 represents the instantaneous signal voltages at the receiver from two independent diversity paths. For the sake of simplicity and in order to reduce the number of variables the noise power N is assumed to be unity. Therefore (11) may be written as

$$SNR_{V_{sel}}|_{N=1} = \max(z_1, z_2) \quad (11)$$

The probability density functions (pdfs) of voltage signal to noise ratio or power signal to noise ratio at the output of the selection combiner are required to evaluate the system performances. In this regard the pdf of the voltage signal to noise ratio is first evaluated by setting the noise power to unity. The other pdf's can be eventually obtained from the above pdf by simple transformation of variables.

The voltage signal to noise ratio at the output of the selection combiner is that of the voltage signal to noise ratio of the strongest diversity branch at its input. For a two branch relay diversity system the output voltage signal to noise ratio is that of branch 1 when the voltage signal to noise ratio of branch 2 is less than or equal to that of branch 1 and vice versa. So if the voltage signal to noise ratio at the output of the selection combiner is denoted by s , it may be concluded that atleast one of the diversity branches have the voltage signal to noise ratio equal to s while the others are less than or equal to s .

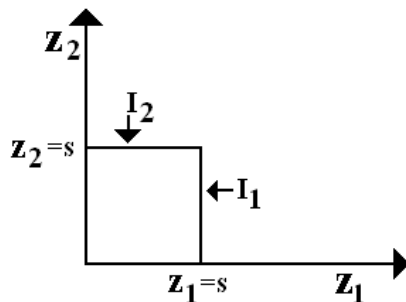


Fig. 6. Combination of values of z_1 and z_2 that forms an envelope s at the output of the selection combiner.

For a two branch diversity system if $z_1 = s$ then $z_2 \leq s$. The line labeled I_1 in Fig. 6. corresponds to this event. The line I_2 corresponds to the situation when $z_1 \leq s$ and $z_2 = s$. The event that the envelope at the output of the selection combiner is s , is the sum of all the events over r_1 and r_2 that produce s as its output. This can be obtained by integrating $f_{Z_1 Z_2}(z_1 z_2)$ along the lines described in Fig. 6. So the envelope at the output of the selection combiner may be written as,

$$f_S(s) = \int_0^s f_{Z_1 Z_2}(z_1 z_2)|_{z_1=s} dz_2 + \int_0^s f_{Z_1 Z_2}(z_1 z_2)|_{z_2=s} dz_1 \quad (12)$$

$$f_S(s) = I_1 + I_2 \quad (13)$$

$$I_1 = \frac{4}{s\Gamma(m_1)\Gamma(m_2)} \left(\frac{s^2 m_1 m_2}{\Omega_1 \Omega_2} \right)^{\frac{m_1+m_2}{2}} \times K_{(m_1-m_2)} \left(2\sqrt{\frac{s^2 m_1 m_2}{\Omega_1 \Omega_2}} \right) \times \frac{4}{\Gamma(m_3)\Gamma(m_4)} \left(\frac{m_3 m_4}{\Omega_3 \Omega_4} \right)^{\frac{m_3+m_4}{2}} \times \int_0^s z_2^{m_3+m_4-1} K_{(m_3-m_4)} \left(2\sqrt{\frac{z_2^2 m_3 m_4}{\Omega_3 \Omega_4}} \right) dz_2 \quad (14)$$

Similarly,

$$I_2 = \frac{4}{s\Gamma(m_3)\Gamma(m_4)} \left(\frac{s^2 m_3 m_4}{\Omega_3 \Omega_4} \right)^{\frac{m_3+m_4}{2}} \times K_{(m_3-m_4)} \left(2\sqrt{\frac{s^2 m_3 m_4}{\Omega_3 \Omega_4}} \right) \times \frac{4}{\Gamma(m_1)\Gamma(m_2)} \left(\frac{m_1 m_2}{\Omega_1 \Omega_2} \right)^{\frac{m_1+m_2}{2}} \times \int_0^s z_1^{m_1+m_2-1} K_{(m_1-m_2)} \left(2\sqrt{\frac{z_1^2 m_1 m_2}{\Omega_1 \Omega_2}} \right) dz_1 \quad (15)$$

In a more compact form the density function at the output of the selection combiner may be written as [7],

$$f_S(s) = C \left\{ s^{m_1+m_2-1} K_{(m_1-m_2)} \left(2\sqrt{\frac{s^2 m_1 m_2}{\Omega_1 \Omega_2}} \right) \cdot \left(\frac{1}{\alpha} \right)^{m_3+m_4} \int_0^{\alpha s} z^{m_3+m_4-1} K_{(m_3-m_4)}(z) dz \right\} + \left\{ s^{m_3+m_4-1} K_{(m_3-m_4)} \left(2\sqrt{\frac{s^2 m_3 m_4}{\Omega_3 \Omega_4}} \right) \cdot \left(\frac{1}{\beta} \right)^{m_1+m_2} \int_0^{\beta s} t^{m_1+m_2-1} K_{(m_1-m_2)}(t) dt \right\} \quad (16)$$

where,

$$C = \frac{16}{\prod_{i=1}^4 \Gamma(m_i)} \left(\frac{m_1 m_2}{\Omega_1 \Omega_2} \right)^{\frac{m_1+m_2}{2}} \left(\frac{m_3 m_4}{\Omega_3 \Omega_4} \right)^{\frac{m_3+m_4}{2}}$$

$$\alpha = 2\sqrt{\frac{m_3 m_4}{\Omega_3 \Omega_4}}$$

$$\beta = 2\sqrt{\frac{m_1 m_2}{\Omega_1 \Omega_2}}$$

Fig. 7. gives the plot of the density functions at the output of the selection combiner for the equation given in (16) as well for the density function obtained through simulation for the same parameters. The m -parameters of all the four links,

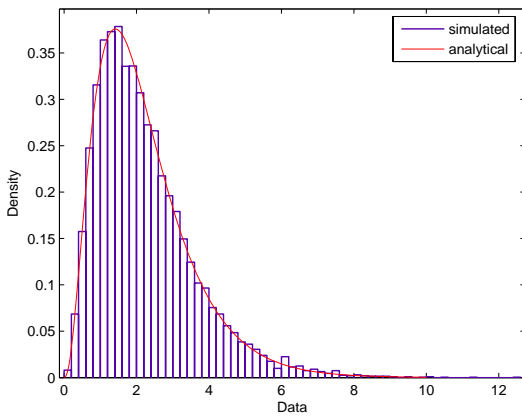


Fig. 7. Pdf of the envelope at the output of a selection combiner.

of the two branches, were set to unity. $\Omega_1, \Omega_2, \Omega_3$ and Ω_4 were taken to be 2. The simulations were done in MATLAB. The Nakagami-m distributed random variables were generated following the procedure given in [8]. Selection at the receiver was done based on the signal strengths.

$f_S(s)$ gives the voltage signal to noise ratio at the output of the selection combiner assuming the noise power to be unity. The power signal to noise ratio is of more relevance and can be obtained from $f_S(s)$ by simple substitution of variables.

The power signal to noise ratio and the voltage signal to noise ratio are related as,

$$SNR_P|_{N=1} = (SNR_V|_{N=1})^2 \quad (17)$$

$$w = s^2 \quad (18)$$

The probability density function of w can be obtained from that of s [10]

$$f_W(w) = \frac{1}{2\sqrt{w}} f_S(\sqrt{w}) + \frac{1}{2\sqrt{w}} f_S(-\sqrt{w}) \quad (19)$$

Since the pdf of s exists only for the positive values, hence the second term of (19) is zero.

$$f_W(w) = \frac{1}{2\sqrt{w}} f_S(\sqrt{w}) \quad (20)$$

All the above pdf's have been derived for unity noise power. But the pdf of the power signal to noise ratio for any arbitrary noise power is of theoretical importance and can be derived from (19). If w_N represents the signal to noise ratio for any arbitrary power N ,

$$w_N = \frac{w}{N} \quad (21)$$

The pdf of w_N is related to that of w by [10]

$$f_{W_N}(w_N) = N f_W(Nw_N) \quad (22)$$

Substituting (20) in (22)

$$f_{W_N}(w_N) = \frac{\sqrt{N}}{2\sqrt{w_N}} f_S(\sqrt{Nw_N}) \quad (23)$$

on further simplification,

$$f_{W_N}(w_N) = \frac{N}{2\sqrt{w_N}} f_S(\sqrt{w_N}) \quad (24)$$

Combining (24) and (16) we obtain

$$f_{W_N}(w_N) = \frac{C\sqrt{N}}{2\sqrt{w_N}} \left[\left\{ (\sqrt{Nw_N})^{m_1+m_2-1} \cdot K_{(m_1-m_2)} \left(2\sqrt{\frac{Nw_N m_1 m_2}{\Omega_1 \Omega_2}} \right) \left(\frac{1}{\alpha} \right)^{m_3+m_4} \int_0^{\alpha\sqrt{Nw_N}} t^{m_3+m_4-1} K_{(m_3-m_4)}(t) dt \right\} + \left\{ (\sqrt{Nw_N})^{m_3+m_4-1} K_{(m_3-m_4)} \left(2\sqrt{\frac{Nw_N m_3 m_4}{\Omega_3 \Omega_4}} \right) \left(\frac{1}{\beta} \right)^{m_1+m_2} \int_0^{\beta\sqrt{Nw_N}} t^{m_1+m_2-1} K_{(m_1-m_2)}(t) dt \right\} \right] \quad (25)$$

where the constants C, α , and β are same as defined in (16).

For $m_1=m_2=m_3=m_4=1$ and $\Omega_1=\Omega_2=\Omega_3=\Omega_4=2$, the power signal to noise ratio at the output of the selection combiner may be written as,

$$f_{W_N}(w_N) = \frac{\sqrt{N}}{2\sqrt{w_N}} \left[\left\{ (\sqrt{Nw_N}) K_0(\sqrt{Nw_N}) \int_0^{\sqrt{Nw_N}} t K_0(t) dt \right\} + \left\{ (\sqrt{Nw_N}) K_0(\sqrt{Nw_N}) \int_0^{\sqrt{Nw_N}} t K_0(t) dt \right\} \right] \quad (26)$$

B. Maximal Ratio Combining

In this section, the probability density function of the SNR at the output of a maximal ratio combiner at the destination node of Fig. 4. is evaluated. The individual links are assumed to be Nakagami faded as earlier. The density functions for both voltage signal to noise and power signal to noise ratio are derived. The voltage signal to noise ratio and power signal to noise ratio are denoted as $SNR_{V_{MRC}}$ and $SNR_{P_{MRC}}$ respectively. The two signal to noise ratios are related to each other and to the input signals of the two diversity branches as,

$$SNR_{V_{MRC}} = \sqrt{SNR_{P_{MRC}}} = \frac{1}{\sqrt{N}} \sqrt{z_1^2 + z_2^2} \quad (27)$$

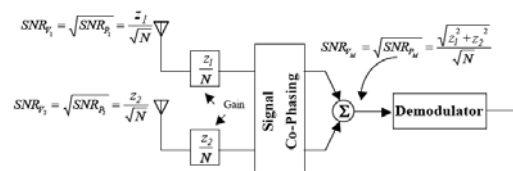


Fig. 8. Block diagram of a two-branch maximal ratio combiner having equal noise power in both the branches.

The joint probability density function of two independent relay channels is as given in (9). It needs to be integrated

to find the probability density function at the output of the maximal ratio combiner. But in Cartesian coordinates the integral becomes very involved. Changing into polar coordinates makes the computations easily tractable. The variables and are written as,

$$z_1 = m \cos \phi \quad (28)$$

$$z_2 = m \sin \phi \quad (29)$$

as, $z_1 \geq 0$ and $z_2 \geq 0$, so $0 \leq \phi \leq \frac{\pi}{2}$. The new probability density function can be deduced from (9), by change of variables and introduction of the Jacobian of the transformation. The new density function is defined as,

$$f_{M\Phi}(m, \phi) = |\tilde{J}| \cdot f_{Z_1 Z_2}(z_1, z_2) \quad (30)$$

where \tilde{J} represents the Jacobian.

$$\tilde{J} = \begin{vmatrix} \frac{\partial z_1}{\partial m} & \frac{\partial z_1}{\partial \phi} \\ \frac{\partial z_2}{\partial m} & \frac{\partial z_2}{\partial \phi} \end{vmatrix} \quad (31)$$

Therefore, (29) gets modified to,

$$f_{M\Phi}(m, \phi) = m \cdot f_{Z_1 Z_2}(z_1, z_2) \Big|_{\substack{z_1 = m \cos \phi \\ z_2 = m \sin \phi}} \quad (32)$$

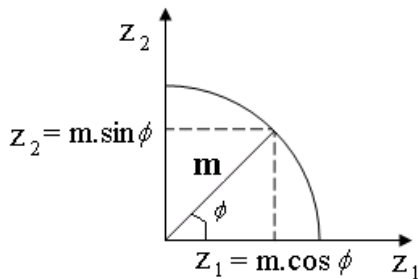


Fig. 9. Combination of values of z_1 and z_2 that forms an envelope m at the output of the maximal ratio combiner.

In (31) ϕ varies from 0 to $\frac{\pi}{2}$. So, $f_M(m)$ may be written as,

$$f_M(m) = \int_0^{\pi/2} f_{M\Phi}(m, \phi) d\phi \quad (33)$$

Substituting (31) into (32),

$$f_M(m) = C m^{m_1+m_2+m_3+m_4-1} \times \int_0^{\pi/2} \frac{1}{\sin \phi \cos \phi} \cos^{m_1+m_2}(\phi) \sin^{m_3+m_4}(\phi) \times K_{(m_1-m_2)} \left(2\sqrt{\frac{m^2 \cos^2(\phi) m_1 m_2}{\Omega_1 \Omega_2}} \right) \times K_{(m_3-m_4)} \left(2\sqrt{\frac{m^2 \sin^2(\phi) m_3 m_4}{\Omega_3 \Omega_4}} \right) d\phi \quad (34)$$

where,

$$C = \frac{16}{\prod_{i=1}^4 \Gamma(m_i)} \left(\frac{m_1 m_2}{\Omega_1 \Omega_2} \right)^{\frac{m_1+m_2}{2}} \left(\frac{m_3 m_4}{\Omega_3 \Omega_4} \right)^{\frac{m_3+m_4}{2}}$$

The density function at the output of the MRC given by (34) requires to be evaluated numerically for specific values of m_i and Ω_i , where $i=1,2,\dots,4$.

For specific case when $m_i=1$ and $\Omega_i = 2$ for $i = 1,\dots,4$. (33) reduces to [11]

$$f_M(m) = C \cdot m^3 \cdot \int_0^{\pi/2} \cos(\phi) \cdot \sin(\phi) \cdot K_0(m \cos(\phi)) \cdot K_0(m \sin(\phi)) d\phi \quad (35)$$

The above integral has been computed numerically to obtain the final density function at the output of maximal ratio combiner as shown in Fig (10).

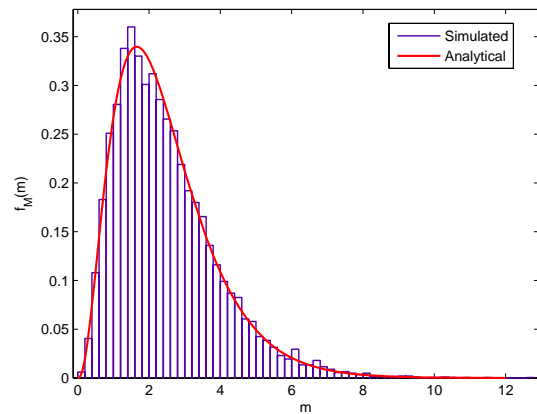


Fig. 10. Pdf of the envelope at the output of the maximal ratio combiner.

IV. BER PERFORMANCE

In Fig. 11. the bit error rate performances for selection and maximal ratio combining in the above mentioned cooperative diversity scheme has been plotted. The simulations were carried out by generating random variables having the density functions given by (16) and (35). The random variables were generated by the method of rejection [12].

Fig. 12. plots the bit error rate for the system described in Fig. 4. and having selection combining at the output. The BER obtained for the channel described in eqn. (16) is same as the BER obtained through simulation of the individual channels, generated according to the methods described in [8], and performing selection combining at the output. The plot in Fig. 12 validates the mathematical derivations. The same were performed for maximal ratio combining at the output and the results were found to be satisfactory.

As mentioned earlier, while evaluating the analytical expressions for the pdf of the two hop relay link, the relay node was assumed to be noise free. Such an assumption of an ideal relay

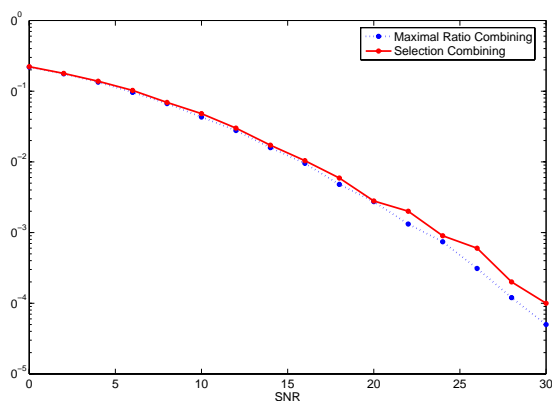


Fig. 11. Plot of bit error rate

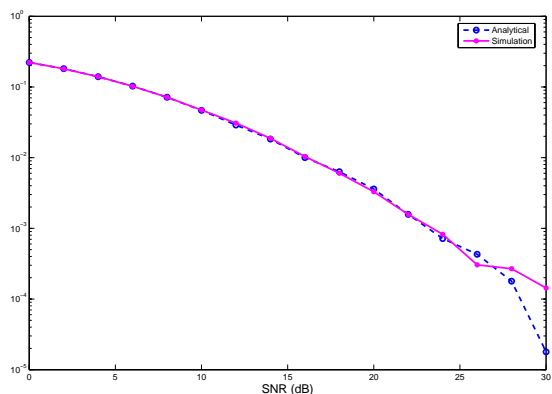


Fig. 12. Comparison of bit error rate obtained analytically and from simulation

was made to reduce the mathematical complexity in derivation of the pdf expression. In practice the SNR at the relay, what so ever large, will be a finite quantity. It is therefore necessary to estimate the error introduced in computation of BER using the pdf in (5) and find some lower limit on the relay SNR above which the error in BER will be reasonably small. To study the behavior of error in link BER as a function of SNR at the relay, we have computed the BER Vs SNR at the destination node with SNR at the relay as a parameter. The range of destination SNR has been taken as 0 - 30dB and the same range has been used for the relay SNR as well. From the knowledge of BER values at different destination SNR for a given SNR at the relay and comparing the same with the BER values those destination SNR's for an ideal relay; we have computed the root mean square (RMS) error in BER at the given relay SNR. The Fig. 13. shows the variation of the RMS error as a function of the SNR at the relay. It may be pointed out that the RMS error estimation can be done more accurately by considering higher SNR ranges as well as evaluating BER at more number of points in the range of the SNR considered. From Fig. 13. one can observe that for the values of relay SNR ≥ 20 dB the equation (5) can be used for computation of BER without making significant error.

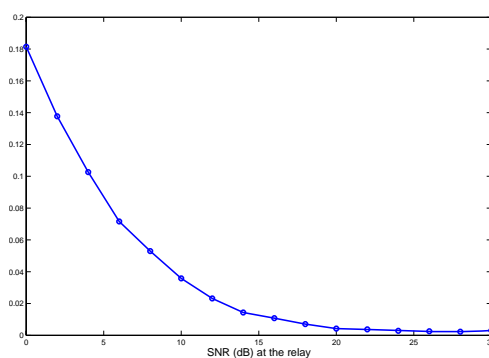


Fig. 13. Root mean square error Vs SNR.

V. CONCLUSION

In this communication we present the closed form expression for the probability density function of the signal envelope at the output of a selection combiner and maximal ratio combiner, having signals from two independent relay channels as inputs. The channel statistics of the individual hops of a relay diversity branch were assumed to be Nakagami-m distributed. We also evaluate the end-to-end density function of a two hop relay branch, with each hop being Nakagami-m distributed. The analytical results were verified through simulation for particular cases. The bit error rates for the two combining schemes (selection combining and maximal ratio combining) were also evaluated for the system shown in Fig. 4.

REFERENCES

- [1] A. Sendonaris, E. Erkip, and B. Aazhang, "User cooperation diversity-part-I: system description," *IEEE Transactions on Communications*, vol. 51, no. 11, November 2003.
- [2] A. Sendonaris, E. Erkip, and B. Aazhang, "User cooperation diversity-part-II: implementation aspects and performance analysis," *IEEE Transactions on Communications*, vol. 51, no. 11, November 2003.
- [3] C. S. Patel, G. L. Stuber, T. G. Pratt, "Statistical properties of amplify and forward relay fading channels," *IEEE Transactions on Vehicular Technology*, vol. 55, no. 1, January 2006.
- [4] M. Nakagami, "The m-distribution-a general formula of intensity distribution of rapid fading," in *Statistical Methods in Radio Wave Propagation*. Oxford, U.K.: Pergamon, 1960, pp. 3-36.
- [5] G.K. Karagiannidis, N.C. Sagias, and P.T. Mathiopoulos, "The N^* nakagami fading channel model," *2nd International Symposium on Wireless Communication Systems*, September 2005.
- [6] I.S. Gradshteyn and I.M. Ryzhik, *Tables of Integrals, Series, and Products*, 5th ed., San Diego, CA: Academic, 1994.
- [7] B. S. Paul and R. Bhattacharjee, "Selection combining of two amplify-forward relay branches with individual links experiencing Nakagami fading," *2007 Asia Pacific Conference on Communication*, Oct. 2007.
- [8] N. C. Beaulieu, "Efficient nakagami-m fading channel simulation," *IEEE Transactions on Vehicular Technology*, vol. 54, no. 2, March 2005.
- [9] W. C. Jakes, *Microwave Mobile Communications*, IEEE Press, 1974.
- [10] V. K. Rohatgi and A. K. Md. Ehsanes Saleh, *An Introduction to Probability and Statistics*. John Wiley & Sons, INC.
- [11] B. S. Paul and R. Bhattacharjee, "Maximal ratio combining of two amplify-forward relay branches with individual links experiencing Nakagami fading," *IEEE TENCON*, Oct.-Nov. 2007.
- [12] W. H. Tranter, K. S. Shanmugan, T. S. Rappaport and K. L. Kosbar, *Principles of Communication Systems Simulation with Wireless Applications*, Prentice Hall, Upper Saddle River, New Jersey.

Babu Sena Paul received his B.Tech and M.Tech degree in Radiophysics and Electronics from the University of Calcutta, West Bengal, India, in 1999 and 2003 respectively. He was with Philips India Ltd from 1999-2000. From 2000-2002 he was lecturer of Electronics and Communication Engineering Dept. at SMIT, Sikkim, India. He is currently pursuing his Ph.D. in the area of wireless communication at IIT Guwahati, Assam, India. He has attended and published several papers in international and national conferences and symposiums. He was awarded the IETE Research Fellowship. He is a life member of IETE.

Ratnajit Bhattacharjee received his B. E. in Electronics and Telecommunication Engineering (First Class Honors) from Gauhati University (REC (at present NIT) Silchar), M. Tech. (E and ECE Department, Microwave Engineering specialization) from IIT Kharagpur and Ph. D. (Engineering) from Jadavpur University Kolkata. Presently he is an Associate Professor in the Department of Electronics and Communication Engineering, IIT Guwahati. Prior to joining IIT Guwahati, he was a faculty member in REC (NIT) Silchar. His research interest includes Wireless communication, Wireless networks, Microstrip antennas, Microwave Engineering and Electromagnetics. He has published over sixty research papers in journals, international and national conferences. He has developed the web course on Electromagnetic Theory under the NPTEL project of MHRD. He has also been involved in several research projects. He has been a Co-investigator for the contracted research from NICT Japan in the area of Next Generation Wireless Networks and currently a member of the research team of the Tiny6 STIC project (funded by French ministry of Foreign Affairs), which deals with IPv6 and Sensor Networks. In NIT Silchar, he was a coordinator for the setting up of Campus Wide Optical Fiber based network under the Centre for Excellence scheme. He was also associated in a number of sponsored projects in the field of development of antenna system. He is a member of IEEE and life member of Indian Society of Technical Education.